Clinical Ophthalmology

Dovepress
open access to scientific and medical research

Open Access Full Text Article

ORIGINAL RESEARCH

ODTiD: Optic Nerve Head SD-OCT Image Dataset

Janarthanam Jothi Balaji[1]
Vasudevan Lakshminarayanan[2]

[1]Department of Optometry, Medical Research Foundation, Chennai, Tamil Nadu, 600006, India; [2]Theoretical and Experimental Epistemology Lab, School of Optometry and Vision Science, University of Waterloo, Waterloo, Ontario, N2L 3G1, Canada

Introduction: Optic disc tilt (ODT) or tilted optic disc is a common finding in the general population. It is due to anomalous development caused by the malclosure of the embryonic optic fissure. ODT is commonly associated with high myopia as well as other conditions. In recent days, the common method to image the optic disc (OD) is by optical coherence tomography (OCT). To the best of our knowledge, there are no datasets of ODT available in the public domain. This dataset aims to make open access raw ODT OCT images to test out new image processing segmentation algorithms.

Methods: This dataset of ODT images contains both horizontal and vertical cross-sectional images obtained using spectral-domain optical coherence tomography (SD-OCT, Cirrus 5000, Carl Zeiss Meditec Inc., Dublin, CA). The optic disc cube 200×200 program was used and all the images are aligned with the center of the optic nerve head. This dataset includes images from both clinically normal (20 eyes) and myopic subjects (101 eyes).

Results: The dataset consists of clear (121) and manually marked (121) images resulting in a total of 242 images. The age distribution for all subjects combined is 27.24 ± 9.28 (range, 11.0–69.0) years. For normal subjects mean ± SD age distribution is 32.40 ± 17.23 years. Similarly, the myopia age distribution is 26.22 ± 6.37 years. Ground truth images, ie, manually segmented by a clinical expert are provided along with other meta-data includes age, gender, laterality, refractive error classification, spherical equivalent (SE), best-corrected visual acuity (BCVA), intraocular pressure (IOP), and axial length (AXL).

Conclusion: This open, public database is online at the ICPSR website of the University of Michigan. The dataset can be used to test and validate newly developed automated segmentation algorithms.

Keywords: optic disc tilt, high myopia, image segmentation, image database, ophthalmology, optical coherence tomography

Introduction

Optic disc tilt (ODT) or Tilted optic disc is a common finding in the general population and is due to anomalous human development[1,2] caused by the malclosure of the embryonic optic fissure.[2,3] High myopia,[1–4] astigmatism,[2] visual field loss,[1,5] defective color vision,[1] and retinal abnormalities are commonly associated with ODT. Usually ODT is considered to be non-progressive[1] except in cases of progressive myopia. The anomalous ODT can be misdiagnosed, as for example, in glaucoma.[1,5] The prevalence of ODT is reported to be the highest (37.0%) amongst myopic Asian subjects.[6]

In myopic eyes with increasing axial length, the optic nerve head loses its original anatomical size and shape.[7,8] In addition to change of the optic disc to

Correspondence: Janarthanam Jothi Balaji
Department of Optometry, Medical Research Foundation, Chennai, Tamil Nadu, 600006, India
Tel +91-44-4227-1500
Fax +91-44-2825-4180
Email jothibalaji@gmail.com

Received: 1 September 2021
Accepted: 11 October 2021
Published: 21 October 2021

a vertical oval shape, a parapapillary gamma zone develops and enlarges at the temporal disc border.[7,8] In eyes with long axial lengths, (>26.0 mm) the Bruch's membrane opening (BMO) diameter increases both horizontally and vertically.[9] Likewise, the Gamma zone may develop due to an axial elongation associated with BMO enlargement.[9] The characteristics of the peripapillary retinal nerve fiber layer (RNFL) thickness is also associated with the degree of temporal myopic ODT.[10,11] Hence, while interpreting the RNFL thickness in myopic eyes the degree of myopic ODT should be considered.[10,11]

The common methods to image the optic disc is by fundus photography, optical coherence tomography (OCT) and confocal scanning laser ophthalmoscopy (Table 1). OCT helps the clinician to image the layers of the retina non-invasively and provides high-speed 3D images of high-quality retinal, optic nerve head, and choroidal vasculature images. OCT images is a useful tool to differentiate true condition/diseases from pseudo status. For example, OCT optic disc images can help in differentiate between true optic disc edema and pseudoedema.[12] Table 1 summarizes the various techniques that have been presented in the literature.

Currently, to the best of our knowledge no imaging instrument has an inbuilt method/algorithm to quantify the ODT. There are many ways to segment the ODT and hence quantify the angle of tilt. Clinicians can use manual or system generated marking. Manual marking is desired but is dependent upon the availability of a trained clinician. In general, during clinical examination the ODT is not quantified due to non-availability of easy methods or tools. Recently, authors presented an automated segmentation ODT algorithm for use with OCT images.[13] The results from this methodology were compared with ground-truth (manually marked by an expert clinician) and the accuracy was reported to be 80.00%.

The availability of real world datasets is essential in accelerating health data science data analytics, including the use of routinely collected data to drive new discoveries and innovations.[45] Khan et al,[45] reported out of 140 unique datasets, 94 raw datasets alone were available for open access. The current paper describes here a dataset for optic nerve head OCT images from myopic subjects. This is to the best of knowledge only dataset dealing with this. This dataset aims to make open access raw ophthalmic ODT OCT images for further analysis and to test out new image processing segmentation algorithms.

Construction and Content

Image Resources

Data from Subjects who visited a tertiary care ophthalmic center in Chennai, India between January 2019 to December 2020 for ophthalmic consultation and underwent OCT imaging are included. All individuals who came for comprehensive ophthalmic examination had signed the written informed general consent agreement prior to their eye examination and approved the use of their data for research purposes. The current study was approved by the IRB of the Vision Research Foundation, Chennai, India and was conducted in accordance with the tenets of the declaration of Helsinki.

The optic nerve head was imaged using a commercially available Spectral-Domain OCT (Cirrus 5000, Carl Zeiss Meditec Inc., Dublin, CA). The optic disc cube 200×200 program was used and all the images were aligned with the center of the optic nerve head. All OCT images were 8-bit grayscale images of dimensions of 200×200 pixels corresponding to 6 mm x 6 mm (894 x 596 pixels). Images with a signal strength of 7 or higher than was included.

Demographic and Clinical Parameters

This dataset consists of a set of optic disc images (vertical and horizontal cross-sectional) from 67 subjects (34 Female, 33 Male) imaged by OCT. These datasets cover both clinical normal and also images of myopic subjects. Table 2, gives details on the dataset which includes 20 healthy normal and 101 myopic OCT images (total 121 images, 60 males, 61 females). These images are divided into three groups: 20 emmetropes (EMM) (SE 0.00 to > −0.50 D), 70 low-moderate myopes (LMM) (SE <-0.50 to −6.00 D), 31 high myopes (HM) (SE <-6.12 D).[46]

In addition to unsegmented optic disc OCT images, the dataset also contains corresponding ground-truth images (each image was manually segmented by an experienced clinician), as well as meta-data, namely age in years, gender, their refractive error as spherical equivalent, refractive classification, BCVA, IOP measured (in mmHg) with Goldmann applanation tonometer, and axial length (in mm) data measured using the non-contact and high-resolution optical biometric device IOLMaster 700 (Carl Zeiss Meditec AG, Jena, Germany).

Characteristics of the Dataset

The Dataset consists of clear (121) and manually marked (121) images resulting in a total of 242 images. These 121 images

Table 1 A Summary of Optic Disc Tilt Assessment Methods

S No	Author (Reference #)	Imaging Method	ODT Quantification Tool	Remarks
1	Gudapati[13]	SD-OCT	Imaging processing	Automated using a ground truth
2	Fraser[14]	SD-OCT	NA	NA
3	Cho[15]	CFP	Deep learning algorithm	Automated using a ground truth
4	Dervisevic[16]	Ophthalmic examination	Descriptively assessed	Clinical observation
5	Chen[17]	CFP	ImageJ	Manual method
6	Park[18]	CFP	ImageJ	Manual method
7	Kim[3]	Swept-Source OCT	NA	Manual method
8	Kosekahya[19]	Ophthalmic examination	Fundus appearance	Clinical observation
9	Choudhury[20]	Stereoscopic FP	NA	Clinical observation
10	Pan[21]	SD-OCT images	NA	Manual method
11	Shoeibi[22]	CFP	Adobe Photoshop CS6	Manual method
12	Marsh-Tootle[23]	SD-OCT images	NA	Manual method
13	Kim[24]	CFP centered on the OD	ImageJ	Manual method
14	Han[5]	CFP	ImageJ	Manual method
15	Sharif[25]	CFP	Adobe Photoshop CS6	Manual method
16	Rebolleda[26]	FP	FP Tilted index	Manual method
17	Sung[27]	OD centered CFP	ImageJ	Manual method
18	Lee[9]	Red-free OD centered FP	ImageJ	Manual method
19	Ando[28]	CFP	NA	NA
20	Hwang[29]	NA	NA	NA
21	Pichi[30]	Stereoscopic FP	FP appearance	Clinical observation
22	Chang[31]	CFP	Adobe Photoshop CS5	Manual method
23	Shinohara[32]	Stereoscopic fundus examination	Fundus appearance	Clinical observation
24	You[33]	SD-OCT images	NA	NA
25	Cohen[34]	CFP	FP appearance	Clinical observation
26	Takasaki[35]	HRT image	HRT printout and ruler	Manual method
27	Kim[36]	CFP	ImageJ	Manual method
28	Hwang[10]	SD-OCT images	ImageJ	Manual method
29	Samarawickrama[6]	Stereo CFP	ImageJ	Manual method
30	Chung[37]	Stereoscopic FP	Adobe Photoshop CS3	Manual method
31	Fledelius[38]	CFP	Slide calipers	Manual method
32	Kaimbo[39]	Ophthalmic examination and FP	FP appearance	Clinical observation
33	You[40]	OD centered CFP	FP appearance	Clinical observation
34	Tong[41]	Stereoscopic OD centered FP	FP appearance	Clinical observation
35	Gürlü[42]	SLP	NA	NA
36	Vongphanit[2]	CFP	Pickett small circles no. 1203	Manual method
37	Gündüz[43]	CFP, FFA & stereoscopic photographs	Planimetric	NA
38	Chihara[44]	Stereoscopic BW photographs	Slide calipers	Manual method

Abbreviations: BW, black and white; CFP, color fundus photography; FFA, fundus fluorescein angiography; FP, fundus photography; NA, not available; OD, optic disc; SD-OCT, spectral-domain optical coherence tomography; SLP, scanning laser polarimetry.

Table 2 Image Details of ODTiD Dataset

	Number of Images*	OD:OS	Gender Ratio (Female: Male)
Emmetropic images	20 X 2	10:10	10:10
Low-Moderate Myopic images	70 X 2	35:35	36:34
High Myopic images	31 X 2	16:15	15:16
Total images	**121 X 2**	**61:60**	**61:60**

Note: *Each subjects image contains both horizontal and vertical images.

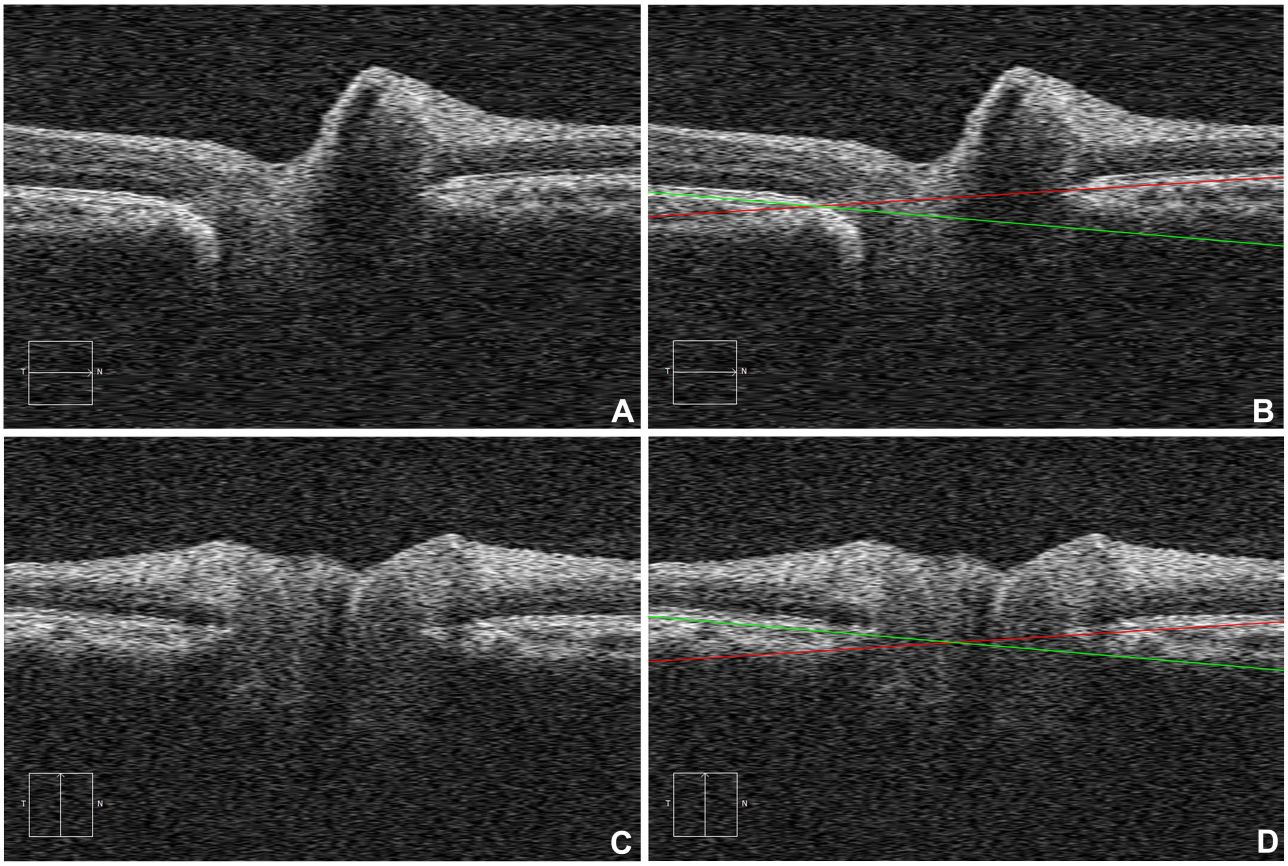

Figure 1 ODT images (**A**) non marked horizontal scanned image, (**B**) manually marked horizontal scanned image (ground truth), (**C**) non marked vertical scanned image, and (**D**) manually marked vertical scanned image.

include patients with myopia (101) and clinically normal (20) images. The age distribution for all subjects combined is 27.24 ± 9.28 (range, 11.0–69.0) years. For normal subjects mean ± SD age distribution is 32.40 ± 17.23 years. Similarly, the myopia age distribution is 26.22 ± 6.37 years.

Manual Marking of Images

Manual marking of all images was done by a trained single clinical expert (JJB). The Cirrus 5000 (Carl Zeiss Meditec Inc., Dublin, CA) provides a cross-sectional image for both horizontal and vertical. The clinician manually drew two straight line aligning the upper boundary RPE layers using a mouse and MS Paint. The boundary line with red-green color used is shown in Figure 1. A caveat should be inserted here - since these boundaries were marked using a mouse it is prone to error because of excessive sliding of the mouse and/or parallax.

Segmentation of RPE Boundary

New segmentation algorithms can be developed using the clear images. Manually marked images can then be used to compare the segmentation achieved with new algorithms. For comparisons the boundary method suggested by Gudapati et al,[13] or other methods can be used. Gudapati et al,[13] for example, introduced various methods and comparisons were then made for each parameter. The source code for the image processing algorithm can be found at https://github.com/gnitish18/OpticDisc-TiltAngle.[13]

Utility and Discussion

Differentiating physiological ODT from a disease involved ODT is clinically important.[12] Recent reports have suggested that optic disc imaging with OCT can improve differential diagnosis involving optic nerve head diseases. Creating and making accessible large and real-world datasets has been essential in accelerating public health database research.[45] To the best of our knowledge this the first publicly available dataset on optic nerve head cross-sectional imaged with OCT. Detailed calculations of ODT parameters from the ODT dataset has been completed and their results have been published elsewhere.[13] These calculations can be used as

a reference for future algorithms. The ODTiD database can be divided into training and test sets for application in machine learning/deep learning methods. This database is available for use by researchers and can be downloaded from the ICPSR website at the University of Michigan (https://doi.org/10.3886/E137701V3).[47] In the future additional marked and non-marked images will be included with their detailed characteristics.

Conclusions

This publicly available, open-access OCT images collection will serve as a dataset for use in biomedical image processing. This dataset will be optimal for researchers aiming to develop quantitative relationships between ODT and pathological conditions such as myopia.

Abbreviations

ODT, The optic disc tilt; SD-OCT, Spectral-domain optical coherence tomography; SE, Spherical equivalent; BCVA, Best corrected visual acuity; IOP, Intraocular pressure; AXL, Axial length; BMO, Bruch's membrane opening; RNFL, retinal nerve fiber layer; OCT, Optical coherence tomography; BW, Black and white; CFP, Color fundus photography; FFA, Fundus fluorescein angiography; FP, Fundus photography; NA, Not available; OD, Optic disc; SLP, Scanning laser polarimetry; EMM, Emmetropes; LMM, Low-moderate myopes; HM, High myopes.

Data Sharing Statement

All the clinical data and materials supporting the manuscript are maintained in our Hospital. This image dataset and clinical parameters are available for use by researchers on the ICPSR website at the University of Michigan (https://doi.org/10.3886/E137701V3).

Ethics Approval and Consent to Participate

This study was approved by the Institutional Review Board of the Vision Research Foundation, Chennai, India. The study conformed to the tenets of the Declaration of Helsinki, and signed informed consent was obtained from all subjects.

Acknowledgments

This work was partly supported by a DISCOVERY Grant from the Natural Sciences and Engineering Research Council of Canada to V. L. The authors thank Mr. V.K. Viekash, for his support in formatting the OCT images.

Funding

There is no funding to report.

Disclosure

The authors declare that they have no competing interests.

References

1. Witmer MT, Margo CE, Drucker M. Tilted optic disks. *Surv Ophthalmol*. 2010;55(5):403–428. doi:10.1016/j.survophthal.2010.01.002
2. Vongphanit J, Mitchell P, Wang JJ. Population prevalence of tilted optic disks and the relationship of this sign to refractive error. *Am J Ophthalmol*. 2002;133(5):679–685. doi:10.1016/S0002-9394(02)01339-9
3. Kim YC, Moon JS, Park HL, Park CK. Three dimensional evaluation of posterior pole and optic nerve head in tilted disc. *Sci Rep*. 2018;8(1):1121. doi:10.1038/s41598-018-19242-z
4. Li Z, Guo X, Xiao O, et al. Optic disc features in highly myopic eyes: the ZOC-BHVI high myopia cohort study. *Optom Vis Sci*. 2018;95(4):318–322. doi:10.1097/OPX.0000000000001200
5. Han JC, Lee EJ, Kim SH, Kee C. Visual field progression pattern associated with optic disc tilt morphology in myopic open-angle glaucoma. *Am J Ophthalmol*. 2016;100(169):33–45. doi:10.1016/j.ajo.2016.06.005
6. Samarawickrama C, Mitchell P, Tong L, et al. Myopia-related optic disc and retinal changes in adolescent children from Singapore. *Ophthalmology*. 2011;118(10):2050–2057. doi:10.1016/j.ophtha.2011.02.040
7. Jonas JB, Ohno-Matsui K, Panda-Jonas S. Myopia: anatomic changes and consequences for its etiology. *Asia-Pac J Ophthalmol*. 2019;8(5):355–359. doi:10.1097/01.APO.0000578944.25956.8b
8. Jonas JB, Wang YX, Dong L, Guo Y, Panda-Jonas S. Advances in myopia research anatomical findings in highly myopic eyes. *Eye Vis*. 2020;2(7):45. doi:10.1186/s40662-020-00210-6
9. Lee JE, Sung KR, Lee JY, Park JM. Implications of optic disc tilt in the progression of primary open-angle glaucoma. *Invest Ophthalmol Vis Sci*. 2015;56(11):6925–6931. doi:10.1167/iovs.15-17892
10. Hwang YH, Yoo C, Kim YY. Myopic optic disc tilt and the characteristics of peripapillary retinal nerve fiber layer thickness measured by spectral-domain optical coherence tomography. *J Glaucoma*. 2012;21(4):260–265. doi:10.1097/IJG.0b013e31820719e1
11. Zhang Q, Xu L, Wei WB, Wang YX, Jonas JB. Size and shape of Bruch's membrane opening in relationship to axial length, gamma zone, and macular Bruch's membrane defects. *Invest Ophthalmol Vis Sci*. 2019;60(7):2591–2598. doi:10.1167/iovs.19-27331
12. Carta A, Mora P, Aldigeri R, et al. Optical coherence tomography is a useful tool in the differentiation between true edema and pseudoedema of the optic disc. *PLoS One*. 2018;13(11):e0208145. doi:10.1371/journal.pone.0208145
13. Gudapati N, Swedha S, Lakshminarayanan V, Jothi Balaji J. Is the optic disc tilt angle different in myopia? *Ophthal Technol XXXI*. 2021;11623:1162328. doi:10.1117/12.2578657
14. Fraser JA, Sibony PA, Petzold A, Thaung C, Hamann S; ODDS Consortium. Peripapillary Hyper-reflective Ovoid Mass-like Structure (PHOMS): an optical coherence tomography marker of axoplasmic stasis in the optic nerve head. *J Neuro Ophthalmol*. 2021. doi:10.1097/WNO.0000000000001203

15. Cho BH, Park KA, Oh SY, et al. Computer-aided recognition of myopic tilted optic disc using deep learning algorithms in fundus photography. *BMC Ophthalmol*. 2020;20(1):1–9. doi:10.1186/s12886-020-01657-w
16. Dervisevic E, Ibrisevic N. Tilted optic disc frequency in myopia of different degree. *Med Arch*. 2019;73(6):391–393. doi:10.5455/medarh.2019.73.391-393
17. Chen Q, He J, Yin Y, et al. Impact of the morphologic characteristics of optic disc on choroidal thickness in young myopic patients. *Invest Ophthalmol Vis Sci*. 2019;60(8):2958–2967. doi:10.1167/iovs.18-26393
18. Park HL, Kim YC, Jung Y, Park CK. Vertical disc tilt and features of the optic nerve head anatomy are related to visual field defect in myopic eyes. *Sci Rep*. 2019;9(1):1–9. doi:10.1038/s41598-019-38960-6
19. Kosekahya P, Sarac O, Koc M, et al. Shifting of the line of sight in tilted disk syndrome. *Eye Contact Lens*. 2018;44(2):S33–S36. doi:10.1097/ICL.0000000000000406
20. Choudhury F, Meuer SM, Klein R, et al.; Chinese American Eye Study Group. Prevalence and characteristics of myopic degeneration in an adult Chinese American population: the Chinese American Eye Study. *Am J Ophthalmol*. 2018;187:34–42. doi:10.1016/j.ajo.2017.12.010
21. Pan T, Su Y, Yuan ST, et al. Optic disc and peripapillary changes by optic coherence tomography in high myopia. *Int J Ophthalmol*. 2018;11(5):874–880.
22. Shoeibi N, Moghadas Sharif N, Daneshvar R, Ehsaei A. Visual field assessment in high myopia with and without tilted optic disc. *Clin Exp Optom*. 2017;100(6):690–694. doi:10.1111/cxo.12511
23. Marsh-Tootle WL, Harb E, Hou W, et al.; Correction of Myopia Evaluation Trial (COMET) Study Group. Optic nerve tilt, crescent, ovality, and torsion in a multi-ethnic cohort of young adults with and without myopia. *Invest Ophthalmol Vis Sci*. 2017;58(7):3158–3171. doi:10.1167/iovs.16-20860
24. Kim YC, Jung Y, Park HL, Park CK. The location of the deepest point of the eyeball determines the optic disc configuration. *Sci Rep*. 2017;7(1):5881. doi:10.1038/s41598-017-06072-8
25. Moghadas Sharif N, Shoeibi N, Ehsaei A, Mallen EA. Optical coherence tomography and biometry in high myopia with tilted disc. *Optom Vis Sci*. 2016;93(11):1380–1386. doi:10.1097/OPX.0000000000000973
26. Rebolleda G, Casado A, Oblanca N, Muñoz-Negrete FJ. The new Bruch's membrane opening - minimum rim width classification improves optical coherence tomography specificity in tilted discs. *Clin Ophthalmol*. 2016;10:2417–2425. doi:10.2147/OPTH.S120237
27. Sung MS, Kang YS, Heo H, Park SW. Characteristics of optic disc rotation in myopic eyes. *Ophthalmology*. 2016;123(2):400–407. doi:10.1016/j.ophtha.2015.10.018
28. Ando Y, Inoue M, Ohno-Matsui K, Kusumi Y, Iida T, Hirakata A. Macular detachment associated with intrachoroidal cavitation in non-pathological myopic eyes. *Retina*. 2015;35(10):1943–1950. doi:10.1097/IAE.0000000000000575
29. Hwang JF, Lin CJ. Multilayered optic disc hemorrhages in adolescents. *J Pediatr Ophthalmol Strabismus*. 2014;51(5):313–318. doi:10.3928/01913913-20140715-01
30. Pichi F, Romano S, Villani E, et al. Spectral-domain optical coherence tomography findings in pediatric tilted disc syndrome. *Graefes Arch Clin Exp Ophthalmol*. 2014;252(10):1661–1667. doi:10.1007/s00417-014-2701-8
31. Chang L, Pan CW, Ohno-Matsui K, et al. Myopia-related fundus changes in Singapore adults with high myopia. *Am J Ophthalmol*. 2013;155(6):991–999. doi:10.1016/j.ajo.2013.01.016
32. Shinohara K, Moriyama M, Shimada N, et al. Analyses of shape of eyes and structure of optic nerves in eyes with tilted disc syndrome by swept-source optical coherence tomography and three-dimensional magnetic resonance imaging. *Eye*. 2013;27(11):1233–1241. doi:10.1038/eye.2013.202
33. You QS, Peng XY, Chen CX, Xu L, Jonas JB. Peripapillary intrachoroidal cavitations. The Beijing eye study. *PLoS One*. 2013;8(10):e78743. doi:10.1371/journal.pone.0078743
34. Cohen SY, Dubois L, Nghiem-Buffet S, et al. Spectral domain optical coherence tomography analysis of macular changes in tilted disk syndrome. *Retina*. 2013;33(7):1338–1345. doi:10.1097/IAE.0b013e3182831364
35. Takasaki H, Higashide T, Takeda H, Ohkubo S, Sugiyama K. Relationship between optic disc ovality and horizontal disc tilt in normal young subjects. *Jpn J Ophthalmol*. 2013;57(1):34–40. doi:10.1007/s10384-012-0193-9
36. Kim TW, Kim M, Weinreb RN, et al. Optic disc change with incipient myopia of childhood. *Ophthalmology*. 2012;119(1):21–26. doi:10.1016/j.ophtha.2011.07.051
37. Chung JK, Yoo YC. Correct calculation circle location of optical coherence tomography in measuring retinal nerve fiber layer thickness in eyes with myopic tilted discs. *Invest Ophthalmol Vis Sci*. 2011;52(11):7894–7900. doi:10.1167/iovs.11-7712
38. Fledelius HC, Goldschmidt E. Optic disc appearance and retinal temporal vessel arcade geometry in high myopia, as based on follow-up data over 38 years. *Acta Ophthalmol*. 2010;88(5):514–520. doi:10.1111/j.1755-3768.2009.01660.x
39. Kaimbo DK. Tilted disc syndrome in Congolese patients. *J Fr Ophthalmol*. 2010;33(3):174–177. doi:10.1016/j.jfo.2010.01.012
40. You QS, Xu L, Jonas JB. Tilted optic discs: the Beijing Eye Study. *Eye*. 2008;22(5):728–729. doi:10.1038/eye.2008.87
41. Tong L, Chan YH, Gazzard G, et al. Heidelberg retinal tomography of optic disc and nerve fiber layer in Singapore children: variations with disc tilt and refractive error. *Invest Ophthalmol Vis Sci*. 2007;48(11):4939–4944. doi:10.1167/iovs.07-0585
42. Gürlü VP, Alýmgýl ML. Retinal nerve fiber analysis and tomography of the optic disc in eyes with tilted disc syndrome. *Ophthalmic Surg Lasers Imaging*. 2005;36(6):494–502. doi:10.3928/1542-8877-20051101-10
43. Gündüz A, Evereklioglu C, Er H, Hepşen IF. Lenticular astigmatism in tilted disc syndrome. *J Cataract Refract Surg*. 2002;28(10):1836–1840. doi:10.1016/S0886-3350(02)01424-4
44. Chihara E, Chihara K. Covariation of optic disc measurements and ocular parameters in the healthy eye. *Graefes Arch Clin Exp Ophthalmol*. 1994;232(5):265–271. doi:10.1007/BF00194475
45. Khan SM, Liu X, Nath S, et al. A global review of publicly available datasets for ophthalmological imaging: barriers to access, usability, and generalisability. *Lancet Digit Health*. 2021;3(1):e51–66. doi:10.1016/S2589-7500(20)30240-5
46. Flitcroft DI, He M, Jonas JB, et al. IMI–Defining and classifying myopia: a proposed set of standards for clinical and epidemiologic studies. *Invest Ophthalmol Vis Sci*. 2019;60(3):M20–M30. doi:10.1167/iovs.18-25957
47. Jothi Balaji J, Lakshminarayanan V. Optic nerve head image database (ODTiD). Ann Arbor, MI: Inter-university Consortium for Political and Social Research [distributor]; 2021. doi:10.3886/E137701V3.